Eur. Phys. J. AP **4**, 171–179 (1998)

THE EUROPEAN PHYSICAL JOURNAL APPLIED PHYSICS

Plasma treatment of aqueous solutes: Some chemical properties of a gliding arc in humid air

B. Benstaali[1], D. Moussa[2,3], A. Addou[1], and J.-L. Brisset[3]

[1] Département de Chimie, Université de Mostaganem, Chemin des Crêtes, Mostaganem, Algéria
[2] STMI, 1 rue de la Noue, 91196 Gif-sur-Yvette, France
[3] Laboratoire d'Électrochimie, UFR des Sciences, Université de Rouen, 76821 Mont-Saint-Aignan Cedex, France

Received: 7 April 1998 / Revised: 7 July 1998 / Accepted: 8 July 1998

Abstract. The chemical properties of the gaseous species generated in a humid air gliding arc discharge are investigated. Aqueous solutions are used as the targets exposed to the plasma, and this allows to evidence strong acid and oxidizing effects on various solutes by means of spectrometric or potentiometric methods. The influence of some working parameters such as the input gas flow, the distance from the electrodes to the target or the electrode gap is examined on the chemical transform and simple experimental laws are derived. A general feature is observed for oxidation and suggests the occurrence of an auto-catalytic step in the relevant kinetic mechanism.

PACS. 82.40.Ra Plasma reactions – 52.40.w Plasma interactions – 52.80.Mg Arcs; sparks; lightning

1 Introduction

A plasma usually results from the increase of the energy of a gas provided by various sources, such as electric, magnetic, mechanical (shock waves, ultrasound) thermal or even optical (laser) sources. The energy transfer may be more or less important according to the nature and the characteristics of the source. A part of the gaseous matter is thus changed from the starting molecules or atoms to an electrically neutral mixture of ions (anions and cations) and electrons, involving other heavy species and photons. The relevant chargeless heavy species include molecules, radicals and atoms. The number of ionized species (or, better, the ratio of the ion population over the overall input gas population) depends on the amount of energy brought to the gas, so that plasmas can be classified into ionized or weakly ionized plasmas. The latter ones are usually characterized by the lack of Local Thermodynamic Equilibrium (LTE) between the electrons and the heavy species. The LTE is realized for the so-called "thermal" plasmas and takes place in plasma torches and arcs. We are specially interested in the "cold" plasmas, for which the energy of the electrons is markedly higher than that of the heavy species, and good relevant examples are given by electric discharges in low pressure gases. Between the two limits (*i.e.*, the LTE is realized or not), a particular intermediate family of plasmas is considered which formally belongs to the non-equilibrium plasmas since they take place near the atmospheric pressure and ambient temperature. These low temperature and high pressure plasmas present a particular interest for the technical and industrial points of view since they involve non drastic working conditions. A typical illustration is the corona discharge, but other plasmas belong to this intermediate class of discharges, such as the gliding arc (or "glidarc") discharge [1]. Due to its dual character of thermal and "cold" plasma, the glidarc presents an attractive feature for both scientific and industrial points of view. The scientist is interested in modelizing [2] such an unusual plasma, and the industrial in new treatments performed at atmospheric pressure. Since most of the plasma treatments of materials are related to the chemical properties of the plasmas, these properties appear as a fundamental aspect which must be examined in chemical terms.

The chemical properties of a plasma are obviously related to those of the species present in the plasma. New species also form (*e.g.*, radicals): thus the plasma accordingly presents new chemical properties and an enhanced reactivity. In addition, a part of the gaseous species is raised to some electronically, vibrationally and rotationally excited level. The electronically excited species present a new electron distribution in the orbitals which confers on them new chemical properties such as the Lewis acid character when an orbital gets empty, as illustrated by singlet oxygen. Also, the gaseous species are usually bare, with no surrounding solvent shell: this contributes to involve them in faster reactions and to assign to them an enhanced reactivity compared to the usual chemical processes.

We focus in this paper on the fundamental chemical properties of a plasma induced by a gliding arc discharge in humid air. We report on the Bronsted acid character (*i.e.*, the proton exchange between an acid and its

conjugated base), and complementary on the highly oxidizing effects (*i.e.*, the electron exchange between an electron donor and an electron acceptor) observed on aqueous solutions. We intend to check whether these effects are similar to those resulting from a corona discharge treatment which were already examined [3,4].

2 Experimental

Two diverging electrodes are raised to a convenient voltage fall of several kilovolts, so that an arc occurs between them in the electrode gap (a few millimeters). A gas flow disposed along the axis of the reactor blows the arc and makes it glide along the electrodes before breaking. After breaking, a new arc occurs and the cyclic evolution resumes. A plasma forms between the electrode and results from the interaction between the arc and the surrounding gas. The AC generator delivers a suitable energy: 100 mA; 9 kV.

The present study is devoted to the interactions between a humid air plasma and an aqueous solution, so that the feeding gas provided by an air compressor is water saturated by passing through a bubbling flask (*i.e.*, a Durand flask) filled with water before entering the reactor through a nozzle of known diameter Φ. The nozzles are selected to provide cylindrical gas flows in the reactor. The electrodes are thus disposed vertically, and the plasma laps against the liquid target disposed in front of the electrodes in a thermostatted vessel as already described [5].

Potential, pH, and absorbance measurements of the treated solutions are performed after determined exposure to the plasma and vigorous stirring of the solution. Chemicals are analytical grade reagents purchased from Merck or Aldrich.

3 Results and discussion

Aqueous solutions of suitable solutes are exposed to the plasma under fixed experimental conditions. The treated solution is then examined by means of suitable techniques (*i.e.*, pH, potential or absorbance measurements) to evidence the pertinent modifications induced by the plasma treatments.

3.1 Active species

A puzzling question is the nature of the species generated in the discharge which induce the chemical effects detailed hereafter. Up to now only limited informations based on experimental results are available. They are based on spectral analysis [6] of the plasma by emission spectroscopy and they show the occurrence of OH° and NO°. In addition, results relevant to other cold plasma device suggest that O_3 may also form although the presence of water is not favorable. The occurrence of hydrogen peroxide may also be assumed, since the electric discharge is a classical way of preparation.

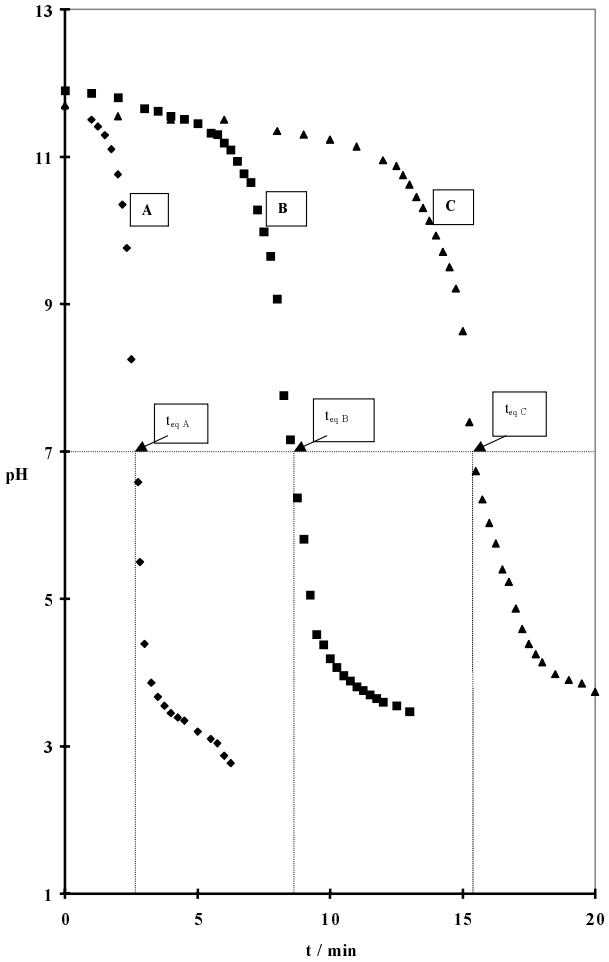

Fig. 1. Plasma neutralization of 125 mL of 5mM NaOH solutions. The pH of the solution depends on the exposure time to the plasma. Experiments are performed at fixed gas flow $Q = 545$ L/min^{-1}, distance $d = 77$ mm and electrode gap $e = 4$ mm but with various nozzle diameters $\Phi = 0.99$ mm (A); 1.5 mm (B) and 2 mm (C).

The presence of water in the gas phase generates OH° and H° radicals. These radicals are involved in the limited oxidation process of NO to NO_2 [7–9]. Also, HO_2° rapidly forms in a three body reaction involving O_2 and H°, as detailed by Van Veldhuizen *et al.* [10] in their study of the reactions of NO in a positive streamer corona plasma.

3.2 Acidity studies

A 125 mL samples of 5 mM NaOH solution are exposed to the plasma. The pH of the solution is measured after stirring for various operating conditions, so that the influence of the major working parameters can be underlined. The pH of the solution decreases as the exposure time t (min) increases and tends to a steady value close to pH = 3. A typical plot of the pH evolution against t is given in Figure 1. In the high pH range, the proton concentration obeys a monologarithmic variation law with t, which is similar to the titration plot of a strong base by a strong

acid and is characterized by the equivalent point t_{eq}. The equivalent points results from the complete neutralization (*i.e.*, pH = 7 in our case) of the OH^- ions of the NaOH solution: it is reached for a plasma treatment of t_{eq} minutes. However, the steady value pH = 3 and positive spot tests for nitrite and nitrate ions suggest the occurrence of the HNO_2/NO_{2-} buffer (pKa = 3.3) in the treated solution. Specific tests for nitrates and nitrites were successful [5].

The value t_{eq} is related to the efficiency of the discharge, since it is related to the number of protons created in the discharge and needed to neutralize the standard NaOH target. It can then be expected that the position of t_{eq} would depend on the main working parameters of the discharge which may be classified as flow, geometry and electric parameters. We are unable to vary the electric parameters since both the voltage and the delivered current are fixed in this study. The forthcoming discussion will thus be limited to the influence of the flow and geometry parameters, and we start by considering the influence of the flow parameters.

3.2.1 Influence of the flow parameters

As illustrated by Figure 1, the position of t_{eq} is affected by the diameter Φ (mm) of the nozzle in the feeding gas system: the smaller is Φ, the smaller is the t_{eq} value. this feature is easily related to the flux of the active species generated in the discharge and able to react with the solute at the plasma/liquid interface. In their study of the corona discharge in humid air, Peyrous *et al.* [11] showed that the occurring molecules N_2, O_2 and H_2O dissociate by electron impact and yield active radicals such as OH°, O_2H° and NO_x, additionally to ozone. These species react with the water vapor over the target solution, and yield more or less dissociated molecules HNO_2 and HNO_3, which drift into the solution where they ionize and dissociate.

For long treatments (*i.e.*, $t > 10$ min), shoulders can be observed on the pH *vs.* t plots. These artefacts can be attributed to the carbonate formation usually observed for the neutralization plots of soda solutions left in ambient air.

Figure 2 shows that t_{eq} is directly correlated with Φ^2 (*i.e.*, $t_{eq} = 4.1386 \times \Phi^2 - 1.324$ with $r^2 = 0.999$) in the investigated Φ range (*i.e.*, $0.99 < \Phi(\text{mm}) < 2$). The flow rate of the feeding gas is the basic flow parameter: its influence on t_{eq} is now examined. A series of "titration" plots performed in the same experimental conditions except the air flow-rate Q (NLh^{-1}) shows that t_{eq} is actually affected by Q: t_{eq} increases as Q decreases. Also t_{eq} is a linear function of Q^{-1} (Fig. 3): $t_{eq} = 11546 \times Q^{-1} - 5.97$ with $r^2 = 0.998$ for $556 < Q$ (NLh^{-1}) < 1250. This result is consistent with those mentioned above: the (constant) number of protons generated by the discharge and needed to neutralize the solution is found in a cylinder of volume $Q^* t_{eq}$, so that t_{eq} is a linear function of Q^{-1}, and of the circular section $\pi^* \Phi^2/4$ of the air jet.

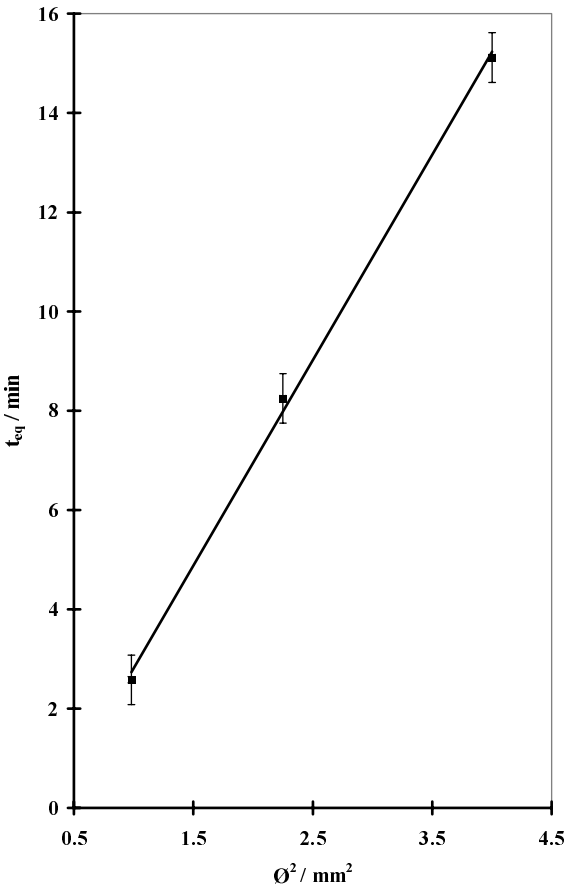

Fig. 2. Correlation between the neutralization time t_{eq} and the square of the nozzle diameter (same experimental conditions as for Fig. 1).

3.2.2 Influence of the geometry parameters

The geometry parameters are the distance d (mm) between the target and the electrodes and the electrode gap e (mm).

The common sense suggests that the activated species generated in the discharge will not be able to reach the liquid surface and react with the solute before they desactivate, so that a decreasing efficiency (*i.e.*, t_{eq}) of the plasma treatment is associated with an increasing distance d. Experimental results confirm the proposal and even a linear correlation is found between t_{eq} and d (Fig. 4): $t_{eq} = 0.0854 \times d + 0.705$ with $r^2 = 0.980$ for $37.5 < d(\text{mm}) < 130$.

The influence of the electrode gap e on t_{eq} can be hardly expected: we can only remind that the larger is e, the longer is the arc, and the more important is the number of active species generated by the discharge. Hence we would conclude in favour of large e values for a high efficiency of the discharge (*i.e.*, a short t_{eq} value). However the arc becomes more and more difficult to establish when e increases too much and becomes higher than a threshold value. Experimental results (Fig. 5) are in good agreement with since the plot t_{eq} *vs.* e presents a minimum around

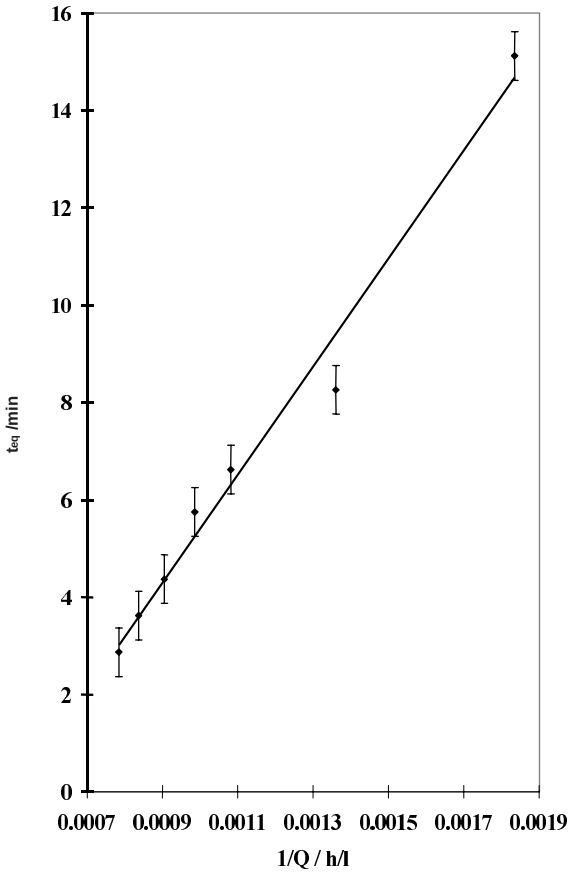

Fig. 3. Influence of the gas flow: t_{eq} *vs.* Q^{-1} (experimental conditions: $\Phi = 2$ mm; $d = 77$ mm; $e = 4$ mm).

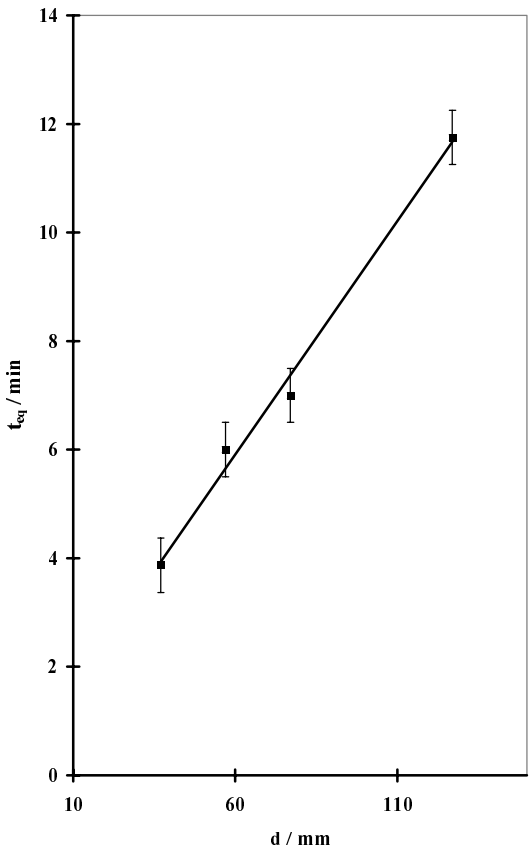

Fig. 4. Influence of the distance d: t_{eq} *vs.* d (experimental conditions: $Q = 925$ Nlh^{-1}; $\Phi = 2$ mm; $e = 4$ mm).

$e = 3$ mm (*i.e.*, $t_{eq} = 0.3575 \times e^2 - 2.5205 \times e + 11.303$ with $r^2 = 0.940$ for $1 < e$ (mm) < 5).

3.2.3 Intermediate conclusion

This limited study of the acid effects induced by a glidarc treatment of aqueous solutions shows a huge acid effect on the target solution, since a pH fall close to 8 units results from a 3 min treatment. This pH fall may be of definite importance in quenching processes of small volumes of solution and in relaxation kinetic studies. The influence of the working parameters, such as the gas flow, the nozzle diameter, the distance from the arc to the target and the electrode gap is examined to determine the more efficient working conditions.

Occurrence of nitrite and nitrate ions as the matching ions to balance the protons formed in the solution was evidenced by spot tests and their concentrations measured [5]. Nitrogen provided by the feeding air is then present in the target solution as oxidized species, which is a strong argument in favor of additional oxidizing processes.

3.3 Oxidation studies

The oxidizing properties are often related to acidity. It is thus natural to check whether this relation holds for a gliding arc and whether solutes in aqueous media also oxidize. We must point out that the oxidizing properties of a gliding arc plasma have already been recognized and used for industrial applications and depollution purposes by Czernichowski *et al.* [12,13], but the authors did not use aqueous targets. We intend in this section to verify that an air plasma still presents marked oxidizing characters towards solutes and to quantify the observed effects. We selected several examples among inorganic and organic compounds to illustrate our purpose.

The oxidizing properties of a gliding arc in humid air can be expected from the gaseous species generated by and in the discharge. Additionally to H_2O_2 for which the electric discharge is among the main techniques to prepare, several highly oxidizing species form, such as ozone (to a limited extent) and various radicals (*e.g.*, OH°, O_2H°) either directly or as products of reactions with water vapor. Some of them are listed in Table 1 which also gathers the standard potentials E° of the involved oxidation-reduction systems. It is striking to see that a number of E° values are close to the oxidation potential of water; this means that the plasma species are able to react with numerous solutes in the aqueous phase and yield the oxidized form

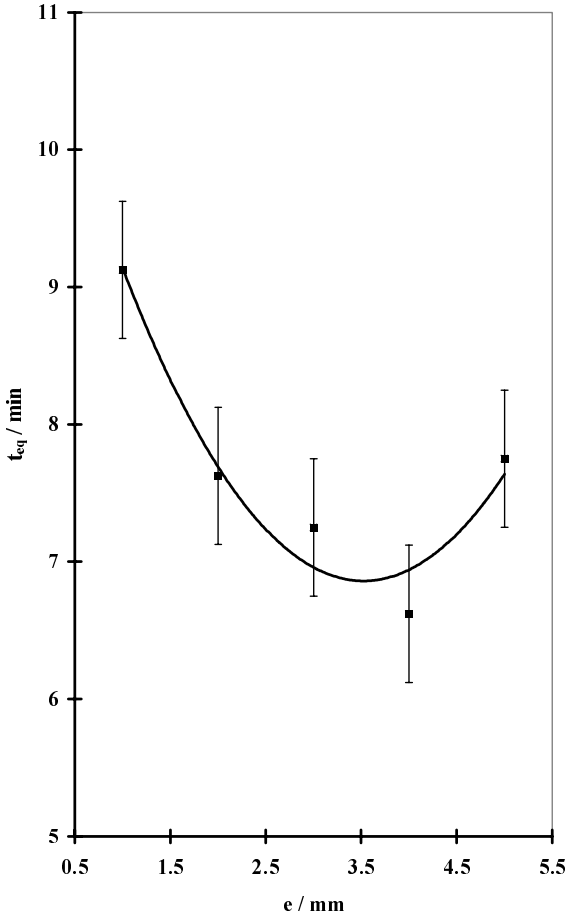

Fig. 5. Influence of the electrode gap e: t_{eq} *vs.* e (experimental conditions: $Q = 925$ Nlh^{-1}; $\Phi = 2$ mm; $d = 77$ mm).

of the solute. We must now get experimental arguments to verify these features.

3.3.1 Oxidation of inorganic solutes

Preliminary experiments were performed on iron derivatives.

For example, the potential of a 0.1 mM aqueous solution of ferrous ions increases with the exposure time and follows a bilogarithmic law. Thus, the oxidation of Fe(II) to Fe(III) observed may be related to the formation of Fenton's reagent since hydrogen peroxide is also involved among the species generated by the discharge.

Oxidation of hexacyanoferrate (II) to hexacyanoferrate (III) can hardly be studied by potentiometry measurements because the formal oxidation potential of the $Fe(CN)_6^{3-}$ / $Fe(CN)_6^{4-}$ system is strongly affected by acidity and increases at low pH. We know from above reported experiments that exposure of the solution to the gliding arc induces a drastic lowering of the pH, thus the conclusions derived from potentiometry measurements may be erratic. To avoid this difficulty, we turned to absorptiometry and measured the absorbance of a 0.1 mM Fe(II) solution at the absorption peak of the oxidized species. The

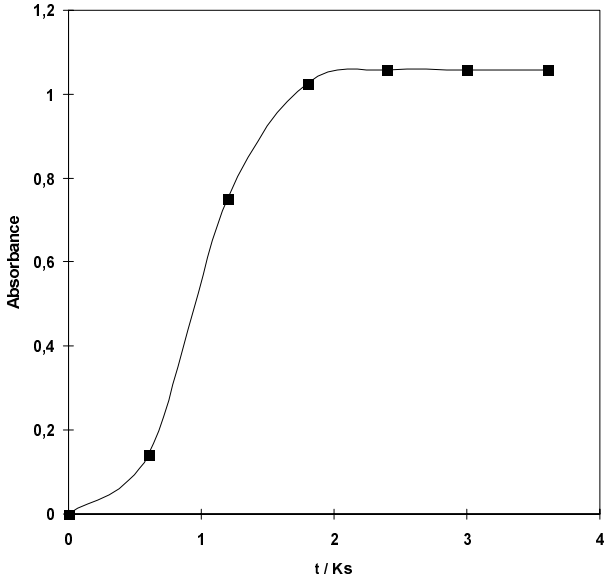

Fig. 6. Evolution with the exposure time $t(\text{min}^{-1})$ to the plasma of the absorbance of a 0.1 mM hexacyanoferrate (II) solution at the absorption peak of the oxidized complex.

absorbance increases with the exposure time and tends to a steady value: its S shape reflects the occurring reaction: $Fe(CN)_6^{4-} \longrightarrow Fe(CN)_6^{3-} + e^-$ and also suggests an auto-catalytic mechanism (Fig. 6). However we must remember that the latter complex is light sensitive and able to yield $Fe(CN)_5(H_2O)^{2-}$, so that the oxidation mechanism and the relevant kinetics cannot be unambiguously interpreted.

Attempts to oxidize ferroïn to ferriïn (*i.e.*, respectively tris(1,10-phenanthroline) Iron(II) and tris(1,10-phenanthroline) Iron(III)) were not successful. The absorbance at the absorption peak (508 nm) of the ferroïn solution decreases on exposing to the plasma and the red colour fades, but the blue colour (absorption peak at 604 nm) of the oxidized complex can be hardly detected. This failure may be related to the huge difference in the ϵ values of the reduced and oxidized complexes which are roughly in the ratio 4×10^4. Also the complex may be destroyed when the ligand oxidize: this may result from the strong oxidizing power of the gas species which are able to attack at the double bonds of aromatic molecules [14].

Oxidation of the ferroïn solution may also be more complex and related with a simplified mechanism involving the following two equilibria [15]:

$$NHO_2 + H^+ + NO_3^- \rightleftarrows 2NO_2 + H_2O \qquad (1)$$

$$NO_2^- + H^+ + Fe(phen)_3^{2+} \rightleftarrows HNO_2 + Fe(phen)_3^{3+}. \qquad (2)$$

We must remember that the plasma treatment enriches the medium with nitrites, nitrates and protons, all species involved in equations (1, 2). According to this mechanism, the ferroïn complex is oxidized to ferriïn by nitrogen dioxide (*i.e.*, a species involving nitrogen at oxidation state (IV)). NO_2 results from the anti-dismutation of N(III) and

Table 1. Selected standard oxidation-reduction potentials (E° / $V, vs.$ NHE)

$O_3 + 2\ H^+ + 2e^-$	$= O_2 + H_2O$	(2.07 V)
$OH^\circ + e^-$	$= OH^-$	(2.02 V)
$H_2O_2 + 2H^+ + 2e^-$	$= 2\ H_2O$	(1.78 V)
$O_2H^\circ + H^+ + e^-$	$= H_2O_2$	(1.50 V)
$O_2 + 4\ H^+ + 4e^-$	$= 2\ H_2O$	(1.23 V)
$2\ HNO_2 + 6H^+ + 6e^-$	$= N_2 + 4\ H_2O$	(1.45 V)
$2\ HNO_{2aq} + 4H^+ + 4e^-$	$= N_2O_{gas} + 3H_2O$	(1.29 V)
$NO_2 + H^+ + e^-$	$= HNO_2$	(1.09 V)
$N_2O_4 + 2H^+ + 2e^-$	$= 2\ HNO_2$	(1.07 V)
$N_2O_4 + 4H^+ + 4e^-$	$= 2\ NO + 2\ H_2O$	(1.03 V)
$HNO_2 + H^+ + e^-$	$= NO + H_2O$	(1.00 V)
$NO_3^- + 4H^+ + 3e^-$	$= NO + 2\ H_2O$	(0.96 V)
$NO_3^- + 3H^+ + 2e^-$	$= HNO_2 + H_2O$	(0.94 V)
$NO_3^- + 2H^+ + e^-$	$= NO_2 + H_2O$	(0.77 V)
$Fe(phen)_3^{3+} + e^-$	$= Fe(phen)_3^{2+}$	(1.06 V)

N(V) described by equation (1). At the juncture, we can point out that the oxidation potentials of the system NO_3^- / NO_2 and NO_2 / NO_2^- are not very different (Tab. 1), which favors the occurrence of equation (1). Oxidation of ferroïn by nitric acid is thus presented [16] as an example of auto-catalytic equilibrium.

The involved auto-catalytic mechanism may also hold for the oxidation of the hexacyanoferrate (II) solution reported above.

0.8 mM iodide solutions were also exposed to the plasma and their absorbance followed as a function of the exposure time. Two bands (at 290 and 350 nm) in the near UV-visible range first appear then disappear (Figs. 7a, 7b), as the color of the sample turns to light yellow then fades to colorless. Figure 8 reports the evolution of these bands with t: for short exposure times, the S shape of the plot agrees with an auto-catalytic effect, with a limited retarding effect. Figure 8 shows the formation and the disparition of an intermediate species identified as I_3^-. We can then guess for the general oxidation mechanism of iodide the occurrence of several steps in relation with the oxidation states of iodine.

$$I^- \longrightarrow I_2 \longrightarrow IO^- \longrightarrow IO_2^- \longrightarrow IO_3^- \longrightarrow IO_4^-$$

$$I(-I) \longrightarrow I(0) \longrightarrow I(+I) \longrightarrow I(+III) \longrightarrow I(+V) \longrightarrow I(+VII).$$

We can conclude from spot tests that the species I(+I), I(+III) and I(+VII) are not present in the solution (even in very small quantities), on the contrary to I(0) and I(+V) species.

Iodine is extracted in chloroform and yields the purple colour characteristic of the iodine complex.

Also, addition of Hg^+, Hg^{2+} and Pb^{2+} ions to the treated solution yields the corresponding iodate precipitates.

Periodates were not detected, neither spectrophotometrically nor by the formation of any silver or baryum precipitate.

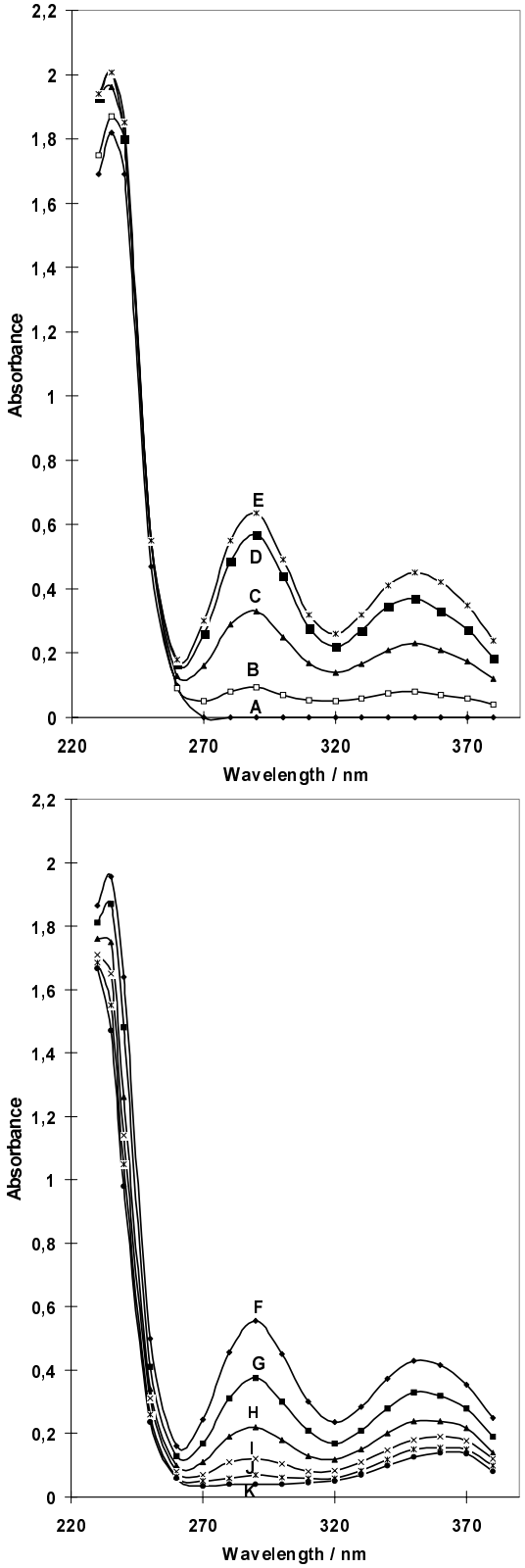

Fig. 7. Evolution with the exposure time t to the plasma of the spectra of a 0.8 mM Iodide solution. Plots (A) to (K) refer to 0 min (A), 1 min (B), 2 min (C), 3 min (D),$\cdots$, 10 min (K) plasma treatments.

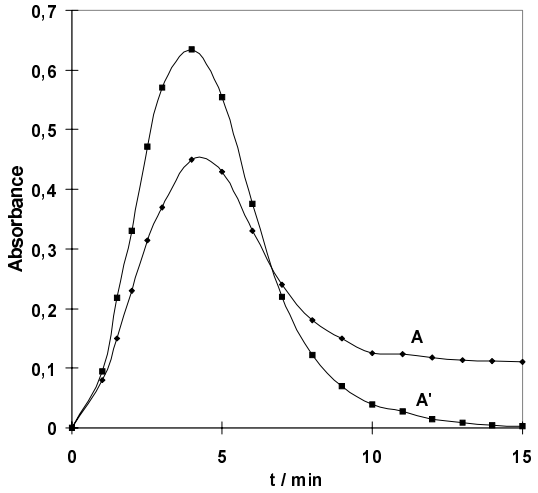

Fig. 8. Evolution with t of the absorbance of a 0.8 mM iodide solution at the absorption peaks of I_3^- at 290 nm (curve A) and 350 nm (curve A').

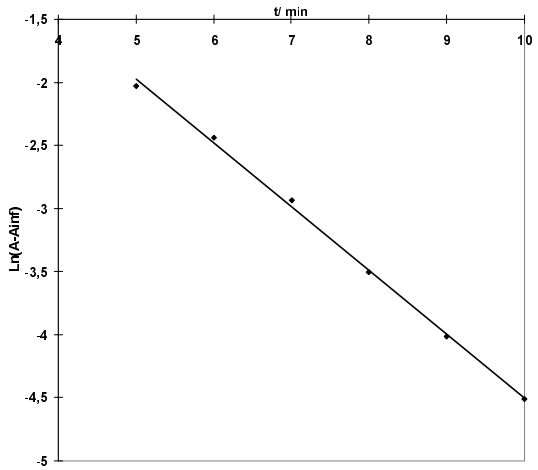

Fig. 9. Logarithm transform of the absorbance A *vs.* t (min) for the removal of I_3^-.

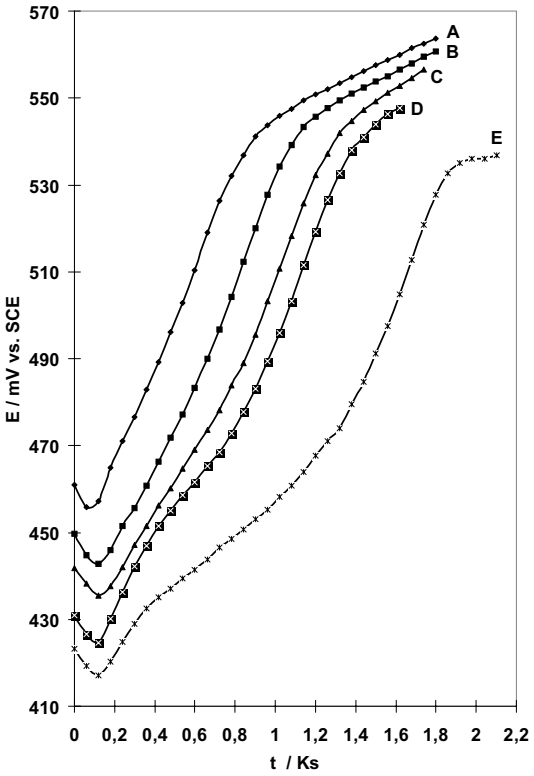

Curve:	A	B	C	D	E
Concentrations:					
$C(I_3^-)$/mM:	0.04	0.1	0.2	0.4	0.8
$C(I^-)$/mM:	0.08	0.2	0.4	0.8	1.6

Fig. 10. Potential E (mV/SCE) changes of iodide/trioidide solutions exposed to the plasma for various times t (kiloseconds). (experimental conditions d = 35 mm; e = 2.5 mm; Φ = 1.5 mm; Q = 16.66 L/min^{-1}).

I(0), I(+I) and I(+III) are well known to rapidly disproportionate to I(−I) and I(+V). IO^- rapidly disproportionate at all temperatures, so that the species is unknown in solution:

$$3IO^- \longrightarrow IO_3^- + 2I^-.$$

IO_2^- is unstable and yields IO_3^-: $3IO_2^- \longrightarrow 2IO_3^- + I^-$.

The Pourbaix diagrams show that I(0) first turns to I(+V) and I(−I) for pH > 7 but stabilizes in acid medium as I_3^-, so that I(0) can be observed as a transient species, which agrees with our observations.

The resulting oxidation mechanism may then be simplified as: I(−I) = I(0) ⟶ I(+V).

Analysis of the absorbance data show that the overall disappearance rate of triiodide I(0) obeys a pseudo first order kinetic law since the logarithm plot $\ln/A_t - A_\infty/vs.\ t$ is linear (Fig. 9). The relevant slope provides the rate of the transform: $k_- = 0.45\ \text{min}^{-1} = 7.5 \times 10^{-3}\text{s}^{-1}$. An estimate of the forward rate for the formation of I(0) gives a value close to k_-(*i.e.*, $k_f = 0.31\ \text{min}^{-1} = 5.17 \times 10^{-3}\text{s}^{-1}$) which is consequent with Figure 8.

Matching series of experiments on the plasma oxidation of iodide was performed and the oxidation of the solute was followed potentiometrically. We added a little quantity of Fe(II) sulphate (2 mM) to a mixture of I^- (30 mM) and I_2 (2 mM) before exposing the solution to the plasma in given working conditions to improve the potentiometric determination of the end point titration of iodide. As expected, the electrode potential (referred to SCE) increases as the exposure time increases (Fig. 10). The E *vs.* t plots are similar to classical titration curves and characterized by the equivalent point for $t = t_{eq}$. For $t < t_{eq}$, the system I(0) / I(−I) governs the potential of the solution, and for $t > t_{eq}$, Fe(II) oxidizes to Fe(III) and the Fe(III)/Fe(II) system fixes the potential, so that the t_{eq} values reflect the working conditions of the plasma treatment. The plots however present a slight minimum for the very beginning of the treatment, and this may be related to the auto-catalytic effect already mentioned.

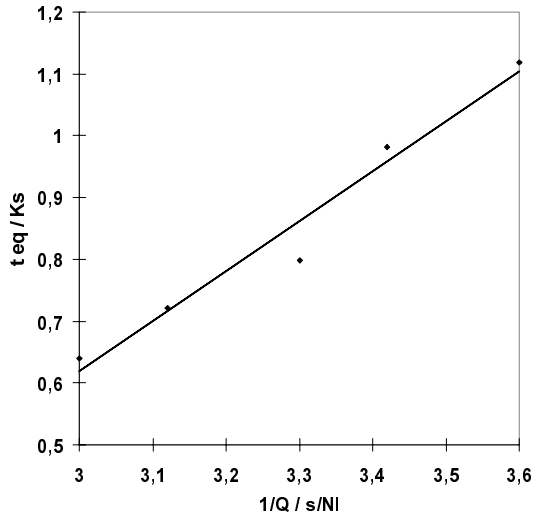

Fig. 11. Variations of t_{eq} *vs.* Q^{-1} for the plasma potentiometric titration of a 0.8 mM iodide solution (same experimental conditions as for Fig. 10).

The influence of the working parameters C, Q and d are then well illustrated by the resulting variations of the t_{eq} values.

For instance varies with the concentration C (mol L^{-1}) of the solute and increases with C. We find that is linearly related to C (*i.e.*, $t_{eq} = 2378 \times C + 10.967$ with $r^2 = 0.981$).

Also depends on the input gas flow Q (NL min^{-1}) and decreases as Q increases (Fig. 11). t_{eq} is a linear function of Q^{-1}($t_{eq} = 815.83 \times Q^{-1} - 30.442$ with $r^2 = 0.987$) as previously observed with the acidity studies.

The characteristic values of the potentiometric curves t_{eq} also reflects the influence of the distance d between the liquid target and the electrodes for given working conditions: t_{eq} linearly increases with d (*i.e.*, $t_{eq} = 5.767 \times d - 1.086$ with $r^2 = 0.956$).

These various correlations are similar to those previously observed in the study of the acid effect, and thus underline the general feature of the gliding arc treatment of solutes.

Complementary experiments were performed in standard conditions of solute concentration, input gas flow and distance d by varying the duration of the "pulse" τ of the exposure to the plasma: t_{eq} increases with τ and tends to a limit. As a first approximation, we may consider that t_{eq} is a linear function of ln τ. This feature may result from a complicated mechanism involving the occurrence of a barrier layer at the gas liquid interface which prevents the active species formed at the surface to drift into the solution and react with the solute.

3.3.2 Oxidation of organic solutes

To enlarge the field of the applications of the gliding arc treatment of solutes, we selected phenosafranine (or safranine T) as a complementary example. This organic dye is also used an an oxidation-reduction indicator and as a biological probe. The pH range covered by the plasma treatment avoids the complications due to possible changes in the bulk protonation state of the starting molecule. Important changes of the solute are induced by the plasma treatment and two kinetic steps are observed from absorbance measurements at 532 nm: they correspond to the formation and the removal steps and may concern the aromatic rings which are sensitive to oxidation.

4 Conclusion

Previous studies were devoted to the behavior of aqueous solutes exposed to the corona discharge in AC or DC conditions, and the main observed effects were reported [3–8]. Chemical analysis of the aqueous targets shows a noticeable acid effect in addition to oxidizing properties. Due to the particular experimental device used for these studies (*i.e.*, a point for the active electrode and a ring-shaped earthed electrode acting as an ion filter) we would conclude that the species responsible for the chemical effects were mainly the neutral species generated at the point electrode and blown away to the solution by the electric wind. We also found that the magnitude of the effects are directly related to the current intensity and the exposure time. This suggests that the quantity of electricity is the basic parameter which generates the chargeless active species.

The chemical effects reported in this paper for the glidarc treatment of solutions are similar to those mentioned for the corona treatment, since large pH and potential jumps are evidenced. We can thus guess that the same effects are associated with the same causes, and assume that the activated neutral species are again responsible for the observed effects. The corona and the glidarc discharges yield "cold" plasmas for which the LTE is not realized. They are also in the same range of input energy. Thus it is reasonable to guess that the same chemical species actually form. This assumption is partly verified since ozone forms as well as hydrogen peroxide, and to a larger extent, nitrous and nitric acids. The oxidation kinetic rates of the latter species are known to be limited in an aqueous medium, and their influence should then be limited in the overall process. The occurrence of OH° radicals was also spectroscopically identified in the glidarc discharge. However a noticeable difference appears between the treatments since the current intensity is much higher for the glidarc than for the corona discharge, which induces more important resulting chemical effects for the glidarc treatment.

The presented study underscores important results of practical interest: an electric discharge in humid air presents highly acid and oxidizing properties towards aqueous solutes. These effects can be used for various applications in liquid treatments, either for the removal of major pollutants from waste waters, or for changing poorly reactive molecules into intermediates of improved reactivity.

References

1. H. Lesueur, A. Czernichowski, J. Chapelle, F. Pat. 2639172 (1988).
2. A. Fridman, R. Petrousov, J. Chapelle, L.M. Canier, A. Czernichowski, H. Lesueur, J. Stevefelt, J. Phys. III France **4**, 1449 (1994).
3. J.-L. Brisset, A. Doubla, J. Lelièvre, J. Amouroux, Analusis **18**, 185-191 (1990).
4. J.-L. Brisset, N. Dubreuil, J. Lelièvre, J. Phys. III France **5**, 447-457 (1995).
5. D. Moussa, J.-L.Brisset, *Proc. 5th Int. symp. on Low Temp. High Pressure Plasmas "Hakone-5"* (Milovy, Czech Rep. 1996), pp. 165-169.
6. B. Benstaali, N.N.A. Addou, B.G. Chéron, J.L. Brisset, (to be published).
7. H. Mazing, Adv. Chem. Phys. LXXX, (J. Wiley, London, 1991).
8. J.S. Chang, J. Aerosol Sci. **20**, 1087 (1989).
9. J.S. Chang, *Non Thermal Plasma Techniques for Pollution Control* NATO ASI Series, edited by B. Penetrante, S. Schultheis **34**, (Springer-Verlag, 1992), pp. 1-32.
10. M.A. Tas, R. van Hardeveld, E.M. van Veldhuizen, Plasma Chem. Plasma Process. **17**, 371 (1997).
11. R. Peyrous, B. Held, P. Pignolet *Papers of Technical Meeting on Electric Discharges*, Tokyo, Aug. 28th, 1987, ED 87-63, pp. 95-109.
12. A. Czernichowski, Pure Appl. Chem. **66**, 1301 (1994).
13. T. Janowski, H.D. Stryczewska, A. Ranaisoloarimanana, A. Czernichowski, *Proc. IUPAC Congress: 12th Int. Symp. Plasma Chem. ISPC-12 825-830* (Minneapolis, USA, 1995).
14. J.L. Brisset, J. Appl. Electrochem. **27**, 179 (1997).
15. G. Bazsa, I. Lengyel, W. Linert J. Chem. Soc. Farad. Trans. 1, **85**, 3273 (1989).
16. M.H. Deniel, D. Lavabre, J.C. Micheau, G. Levy, Bull. Union Phys. **787**, 1503 (1996).